Effects of Deoxygenation on Active and Passive Ca^{2+} Transport and on the Cytoplasmic Ca^{2+} Levels of Sickle Cell Anemia Red Cells

Zipora Etzion,* Teresa Tiffert,‡ Robert M. Bookchin,* and Virgilio L. Lew‡

**Department of Medicine, Albert Einstein College of Medicine, Bronx, New York 10461; and ‡Physiological Laboratory, University of Cambridge, Cambridge CB2 3EG, United Kingdom*

Abstract

Elevated $[Ca^{2+}]_i$ in deoxygenated sickle cell anemia (SS) red cells (RBCs) could trigger a major dehydration pathway via the Ca^{2+}-sensitive K^+ channel. But apart from an increase in calcium permeability, the effects of deoxygenation on the Ca^{2+} metabolism of sickle cells have not been previously documented. With the application of $^{45}Ca^{2+}$-tracer flux methods and the combined use of the ionophore A23187, Co^{2+} ions, and intracellular incorporation of the Ca^{2+} chelator benz-2, in density-fractionated SS RBCs, we show here for the first time that upon deoxygenation, the mean $[Ca^{2+}]_i$ level of SS discocytes was significantly increased, two- to threefold, from a normal range of 9.4 to 11.4 nM in the oxygenated cells, to a range of 21.8 to 31.7 nM in the deoxygenated cells, closer to K^+ channel activatory levels. Unlike normal RBCs, deoxygenated SS RBCs showed a two- to fourfold increase in pump-leak Ca^{2+} turnover. Deoxygenation of the SS RBCs reduced their Ca^{2+} pump V_{max}, more so in reticulocyte- and discocyte-rich than in dense cell fractions, and decreased their cytoplasmic Ca^{2+} buffering. Analysis of these results suggests that both increased Ca^{2+} influx and reduced Ca^{2+} pump extrusion contribute to the $[Ca^{2+}]_i$ elevation. (*J. Clin. Invest.* 1993. 92:2489–2498.) Key words: deoxygenation • sickle cell anemia • red cells • cytoplasmic Ca^{2+} buffering • Ca^{2+} pump • hemoglobin S

Introduction

Circulating sickle cell anemia (SS)[1] red blood cells (RBCs) have a well recognized heterogeneity of age, morphology, volume, composition, membrane structure, and ion transport (1–3). Much of this heterogeneity is the direct or indirect result of the intracellular polymerization of hemoglobin (Hb) S on deoxygenation. Sickling permeabilizes the cell membranes to mono- and divalent cations (2, 4–7) producing secondary abnormalities of RBC ion and water contents. The ion and water shifts are mediated mostly by large-capacity K^+ transporters, such as Ca^{2+}-sensitive K channels and K:Cl carriers, which can both be directly or indirectly stimulated by increased intracellular ionized Ca^{2+} concentration ($[Ca^{2+}]_i$), resulting in rapid net loss of KCl and water (8).

SS RBCs have abnormally high total calcium contents ($[Ca_T]_i$) (9, 10), which is lowest in the light, reticulocyte-rich cell fraction containing the youngest RBCs, higher in the middle-density discocyte-rich fraction, and highest in the densest RBCs, predominantly irreversibly sickled cells (ISC; reference 11). The elevated calcium is contained within intracellular vesicles capable of ATP-dependent Ca^{2+} accumulation (12–14). Normal (AA) RBCs also have endocytic vesicles, whose substantial calcium accumulating capacity can be demonstrated experimentally by increasing the Ca^{2+} permeability of the outer cell membrane (12); but these RBCs are virtually calcium-free (15, 16). These comparisons suggest that an increase in Ca^{2+} permeability is a prerequisite for calcium accumulation within RBCs, and that either the Ca^{2+} permeability of normal RBCs is not increased in the circulation or else that vesicles with accumulated calcium are rapidly and selectively removed. Since SS RBCs have normal Ca^{2+} permeability in the oxygenated (oxy) state in vitro (2), their calcium accumulation must result from deoxygenation-induced episodes of increased Ca^{2+} permeabilization in the circulation, with transient elevations of $[Ca^{2+}]_i$.

Despite growing evidence for its relevance in triggering SS RBC dehydration, this predicted deoxygenation-induced increase in $[Ca^{2+}]_i$ had not yet been successfully measured (17). We recently showed (18) that in AA RBCs, deoxygenation reduced both the saturated Ca^{2+} extrusion rate through the Ca^{2+} pump (V_{max}) and the cytoplasmic Ca^{2+} buffering. Those results prompt the additional question of whether Ca^{2+} pump inhibition might also occur in deoxygenated (deoxy) SS RBCs and, together with the observed increase in Ca^{2+} permeability, could contribute to an elevated $[Ca^{2+}]_i$ in those cells. The present study examines the effects of deoxygenation on the Ca^{2+} pump V_{max} of density-separated SS cell fractions, and on the pump-leak Ca^{2+} fluxes and $[Ca^{2+}]_i$ levels of SS discocytes.

Methods

Composition of solutions. Solution A contained, in mM: KCl, 80; NaCl, 70; $MgCl_2$, 0.15; Na-Hepes, pH 7.4–7.5 at 37°C, 10, and NaOH-neutralized EGTA, 0.1. Solution B was the same as solution A but without Na-EGTA. Solution C was the same as solution B but contained, in addition, 10 mM inosine. A 40 mM $^{45}CaCl_2$ stock solution was prepared, with specific activity of $^{45}Ca^{2+}$ between 8×10^6 and 6×10^7 cpm/μmol. Note that the high-K suspending media with 0.15 mM $MgCl_2$ prevents those changes in RBC volume, ion content, and pH that occur after exposure to divalent cation ionophores in the presence of Ca^{2+}, due to Ca^{2+}-induced K^+-permeabilization (19–21).

A preliminary report of portions of this work was published in abstract form (1992. *Blood.* 80:77*a*).

Address correspondence to Dr. Robert M. Bookchin, Department of Medicine, Albert Einstein College of Medicine, 1300 Morris Park Avenue, Room 913U, Bronx, NY 10461.

Received for publication 22 February 1993 and in revised form 16 May 1993.

1. *Abbreviations used in this paper:* deoxy, deoxygenated; Hb, hemoglobin; ISC, irreversibly sickled cell; oxy, oxygenated; SS, sickle cell anemia or homozygous hemoglobin S disease.

J. Clin. Invest.
© The American Society for Clinical Investigation, Inc.
0021-9738/93/11/2489/10 $2.00
Volume 92, November 1993, 2489–2498

Preparation of density-fractionated SS RBCs. Heparinized venous blood was obtained after informed consent from sickle cell anemia patients with established genotype, and kept at 4°C for no more than 1 h before processing, to isolate RBC density fractions as previously described (22, 23). Briefly, after centrifugation (2000 $g \times 10$ min), plasma was removed and the packed cells were filtered through a nylon mesh (20 μm, Nitex nylon; Tetko Inc., Lancaster, NY) to remove white cells with minimal loss of reticulocytes. The RBCs were washed thrice in solution A, with filtering after each wash, resuspended in A at ~ 40% hematocrit (Hct), and layered onto a discontinuous gradient of arabinogalactan (Larex-L.O.; Consulting Associates, Inc., Tacoma, WA) using three density (δ) layers, 1.087, 1.091, 1.118, and a cushion of δ = 1.170. Four fractions of RBCs were harvested: cells with $\delta \leq 1.087$ (R1) and with $1.087 < \delta \leq 1.091$ (R2) were rich in reticulocytes (R2 usually had fewer than R1); cells with $1.091 < \delta \leq 1.118$ were primarily discocytes (D), and the dense cells, with $\delta > 1.118$, were mainly ISC. The RBCs were washed twice in solution A and twice in solution B before use in the procedures below.

Measurement of Ca^{2+} pump V_{max}. The effect of deoxygenation on the V_{max} of the Ca^{2+} pump was measured by the method of Tiffert et al. (18). Briefly, density-fractionated SS RBCs were suspended at about 10% Hct in solution C, and 2 ml of each RBC suspension were equilibrated in a tonometer (model 237; Instrumentation Laboratory Inc., Lexington, MA) at 37°C with water-saturated oxygen (O_2) or nitrogen (N_2) gas for about 10 min. 5 μl of the 40 mM $^{45}CaCl_2$ stock solution were added to the suspension during this period, to give a final total calcium concentration in the suspension ($[Ca_T]_s$) of about 100 μM. At t = 0, 10 μl of a 2 mM A23187 stock solution in ethanol:DMSO (4:1) were added to give a final concentration of 100 μmol/l RBCs (since most of the ionophore forms partitions in the cells' membrane [24, 25]). After 2 min, 5 μl of a 70 mM $CoCl_2$ solution were added to the RBC suspension to give ~ 200 μM final Co^{2+} concentration, which blocks all passive fluxes of Ca^{2+} through the ionophore, with no significant effects on Ca^{2+} pump fluxes (26). Frequent 50 μl samples were taken after ionophore and Co^{2+} additions, as indicated in the Figs. 1–4 and processed for measurement of $[Ca_T]_i$, as described previously (26). Triplicate 20 μl samples of each cell suspension were mixed with 1 ml Drabkin's reagent for spectrophotometric measurement of Hb as cyanmetHb.

Estimates of cytoplasmic Ca^{2+} buffering. These were performed on the measurements reported in Fig. 3 (oxy RBCs only), and refer to results in Table IV. The method analyzes transmembrane Ca^{2+} equilibria induced by the divalent cation ionophore A23187, a specific M^{2+}:$2H^+$ exchanger (27). The above concentrations of A23187 (~ 100 μmol/l cells) mediate RBC Ca^{2+} fluxes far beyond those of saturated Ca^{2+} pumps, ensuring rapid and nearly total Ca^{2+} equilibration, even in substrate-fed cells (28, 29) (see Fig. 1). The ionophore-induced equilibrium is given by:

$$([Ca^{2+}]_i)_{Eq}/([Ca^{2+}]_o)_{Eq} = ([H^+]_i/[H^+]_o)^2 = r^2 \text{ (reference 27)},$$

where $([Ca^{2+}]_i)_{Eq}$ and $([Ca^{2+}]_o)_{Eq}$ are the intra- and extracellular concentrations of ionized calcium at equilibrium, and r is the intra- to extracellular proton concentration ratio. The fraction of total RBC calcium which is in ionized form, α, is defined by (references 19 and 20):

$$\alpha = ([Ca^{2+}]_i)_{Eq}/([Ca_T]_i)_{Eq},$$

where $([Ca_T]_i)_{Eq}$ is the total RBC calcium concentration at equilibrium. By dividing these two equations, we obtain (reference 19):

$$r^2/\alpha = ([Ca_T]_i)_{Eq}/([Ca^{2+}]_o)_{Eq}$$

from which α can be estimated by measuring r and the ionophore-induced equilibrium concentrations of Ca^{2+} in the medium ($([Ca^{2+}]_o)_{Eq}$) and of total calcium in the RBCs ($([Ca_T]_i)_{Eq}$). Thus,

$$\alpha = r^2/(([Ca_T]_i)_{Eq}/([Ca^{2+}]_o)_{Eq}).$$

An estimate of r in representative oxy and deoxy suspensions of density-fractionated SS RBCs was obtained by measurements of suspension pH (pH_s; preliminary measurements showed that with the low Hct suspensions used, pH_s and medium pH (pH_o) were not distinguishable) and of intracellular pH (pH_i). For measurements of pH_i, RBC suspensions were spun for 2 min in a microcentrifuge (on deoxy cells, the suspensions were transferred with a gas-tight syringe to the microcentrifuge tubes under oil); after removal of the supernatant, the packed RBC were frozen and thawed in liquid nitrogen and (after aspiration of the oil if present) the hemolysate pH was measured at 37°C using a Radiometer PHM 71 MK2 meter and a glass microcapillary electrode unit, type E5021a. Medium pH (pH_o) was measured with the same electrode at 37°C. These measurements provide $r = [H^+]_i/[H^+]_o$. With the deoxygenated dense SS red cells, pH_i could not be measured this way because of the high viscosity of the cytoplasm; as noted in the legend of Table IV, the r value for the ISC fraction was taken as the mean of several previous measurements made determining the chloride ratio $[Cl^-]_o/[Cl^+]_i$ directly using a chloridometer (7).

Measurement of the pump-leak turnover of Ca^{2+} and steady-state $[Ca^{2+}]_i$ in SS RBCs. The effect of deoxygenation on the physiological pump-leak turnover of Ca^{2+}, and on $[Ca^{2+}]_i$, was measured by the method of Lew et al. (30). The RBCs were preloaded nondisruptively with the high affinity Ca^{2+} chelator benz-2 by incubation for 90 min at 37°C with the acetomethoxy derivative (benz-2-AM) in the presence of 5 mM sodium pyruvate to bypass the ATP-depleting effects of formaldehyde released during benz-2 incorporation (31–33). These experiments were done only with the SS discocyte fractions (D), because the cells were sufficiently abundant, and because, unlike the cells from reticulocyte-rich fractions, they were found to withstand the prolonged benz-2 loading and postincubation procedures with minimal lysis. The RBCs were suspended at 10% Hct in autologous plasma containing 5 mM sodium pyruvate and 5 mM inosine, and equilibrated in the tonometer with humidified N_2 or O_2, each containing 5.6% CO_2. Intracellular benz-2 concentrations were estimated on aliquots of RBCs rapidly depleted of ATP by incubation with inosine and iodoacetamide and suspended in solution B with added $^{45}Ca^{2+}$ and EGTA, as described previously (30, 31). The intracellular concentration of benz-2 ($[benz\text{-}2]_i$) was obtained from the equilibrium distribution of $[Ca_T]_i/[Ca_T]_o$ induced by the ionophore A23187 (31).

Results

Effects of deoxygenation and SS RBC density on ionophore-induced Ca^{2+} distribution and on Co^{2+}-exposed Ca^{2+} efflux through the Ca^{2+} pump. The results of typical experiments are shown in Figs. 1–3, and the combined Ca^{2+} efflux results from four experiments are reported in Table I. The protocol followed in these experiments can be seen in Fig. 1. The ionophore was added at $t = 0$ to induce a large Ca^{2+} load and after 2 min, Co^{2+} was added, which blocks the ionophore-induced Ca^{2+} permeability, and exposes the uphill Ca^{2+} efflux through the Ca^{2+} pump. In the experiment of Fig. 1, Ca^{2+} efflux was followed for 2 min to allow estimate of V_{max}; in that of Fig. 2, Ca^{2+} efflux was followed for 10 min (after adding Co^{2+}) to assess, besides V_{max}, whether the tail-off pattern of the Ca^{2+} efflux curves differed among the various RBC density fractions.

The results showed that: (*a*) addition of ionophore triggered a rapid net Ca^{2+} influx of 30 to 70 mmol/(340 g Hb h), which led to near Ca^{2+} equilibration across the membrane within about 60–90 s in all density fractions (Fig. 1); (*b*) in each RBC fraction, the total cell calcium content at equilibrium ($([Ca_T]_i)_{Eq}$) was lower in deoxy than in oxy conditions (Figs. 1 and 3); (*c*) $([Ca_T]_i)_{Eq}$ declined with increased RBC density (Figs. 1 and 3); (*d*) Ca^{2+} pump V_{max} in oxy conditions showed moderate variation, both among RBCs from different donors, as seen before with normal (AA) RBCs (26), and also

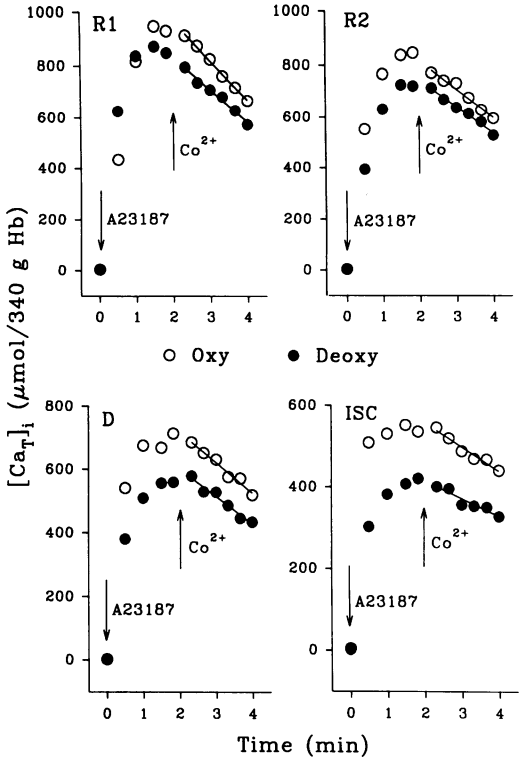

Figure 1. Effects of deoxygenation on ionophore-induced Ca^{2+} equilibration and on the V_{max} of the Ca^{2+} pump in four SS RBC fractions. $[Ca_T]_i$ is plotted as a function of time in oxy and deoxy conditions. A23187 was added at time 0, and Co^{2+} at 2 min. V_{max} values were obtained as the initial Ca^{2+} effluxes after Co^{2+} addition, from the slopes of first order regression lines through those experimental points (see lines). All correlation coefficients were > 0.9. This experiment corresponds to donor 3 in Table I.

among the different RBC fractions from the same donor; there was no consistent pattern in this variation, except for a tendency to lower values in the ISC-rich cell fraction than in the discocyte fraction of the same donor (Table I); (*e*) deoxygenation of SS density fractions from four donors resulted in a modest reduction in Ca^{2+} pump V_{max} which was significant for the reticulocyte-rich fraction and discocyte fractions, but inconsistent in the dense SS cells (Table I); (*f*) the tail-off pattern of the Ca^{2+} efflux curves differed among the SS RBC fractions, as seen in the curves of $[Ca_T]_i$ vs. time in the experiment of Fig. 2, and in two additional experiments (not shown), in the following way: With the R1 fraction, the late reduction in the slope of the Ca^{2+} efflux curve began at the highest $[Ca_T]_i$ level and showed the most gradual further reduction; the extent of these features followed the sequence R1 > ISC ≥ R2 > D. This tail-off pattern is compatible with retention of Ca^{2+} in intracellular pools (12, 34), maximal in the light SS reticulocytes and least in the discocytes.

Deoxygenation-induced pH changes. Deoxygenation of RBC suspensions alkalinizes both the cells and medium due to the binding of Bohr protons to deoxy-Hb (35, 36). These pH shifts must be measured to assess their possible contribution to the observed changes in Ca^{2+} pump V_{max} on deoxygenation. The approach used in our recent studies of AA RBCs (18) was applied here to SS RBCs.

Isoelectric focusing of pure Hb A and S solutions had shown that the pI of human Hb A increases on deoxygenation from 6.95 to 7.10 (35), and that of Hb S from about 7.2 to 7.35. These are both increased by 0.15 units. The method provided reliable oxy-deoxy differentials, but only approximate absolute values (Bunn, H. F., personal communication). When intact AA RBCs were deoxygenated, analysis of the observed pH shifts, using a modification of our red cell model (18), suggested that the oxy–deoxy ΔpI of Hb A was between 0.2 and 0.4 units. The results of a similar analysis of SS RBCs are shown in Table II, which compares measured and predicted changes in cell and medium pH on deoxygenation of SS RBCs in one representative experiment. The observed deoxy-induced pH_i changes in eight similar experiments of this series could be accounted for by an oxy–deoxy ΔpI of 0.172±0.013 (mean±SEM), with a range of 0.13 to 0.23, not significantly different from that obtained in pure solutions of Hb A or S.

Effect of deoxygenation on passive Ca^{2+} influx and pump-leak steady-state $[Ca^{2+}]_i$ level in SS discocytes. The results of three similar experiments are shown in Table III. In agreement with earlier results (2, 13, 17), deoxygenation of unfractionated SS RBCs or the discocyte fraction alone was associated with a three- to fivefold increase in passive Ca^{2+} influx. The main new finding was the documentation of a substantial increase in $[Ca_T]_i$, and therefore in $[Ca^{2+}]_i$, in the pump-leak steady-state of the deoxy SS discocytes. These results are distinctly different from those recently obtained with AA RBCs

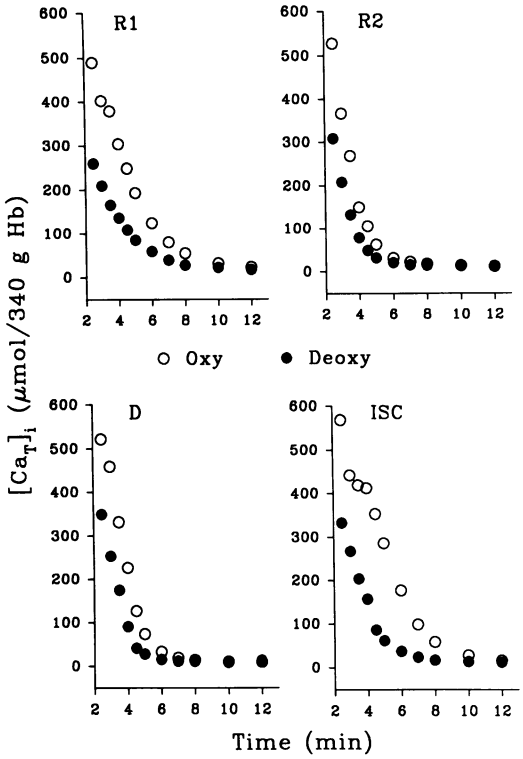

Figure 2. Effect of deoxygenation on the Co^{2+}-exposed Ca^{2+} pump efflux from SS RBC fractions. $[Ca_T]$ is plotted as a function of time in oxy and deoxy conditions. Ca^{2+} efflux (against an inward Ca^{2+} gradient) was followed for 10 minutes after Co^{2+} addition to detect differences in tail-off pattern among the fractions. The results are representative of three similar experiments. This experiment corresponds to donor 2 in Table I. Note that in this experiment, unlike that in Figs. 1 and 3, in which samples were taken to determine $([Ca_T]_i)_{Eq}$, the initial (2 min) measurements of $[Ca^T]_i$ do not represent equilibrium values.

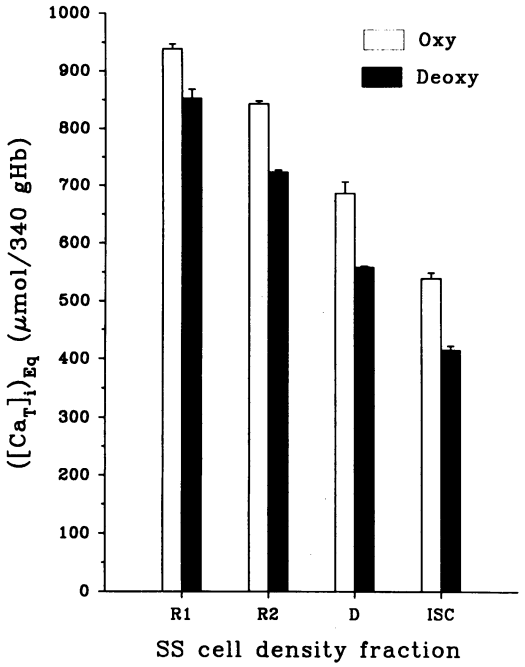

Figure 3. Effect of deoxygenation on the A23187-induced total cell calcium content at equilibrium, $([Ca_T]_i)_{Eq}$, in SS RBC fractions. This experiment corresponds to donor 3 in Table I, and the results are also plotted in Fig. 1. The values were derived from the means of the two or three maximal values of $[Ca_T]_i$ in the experiments of Fig. 1, just before addition of Co^{2+}. The error bars report±SEM.

(18), in which deoxygenation did not significantly alter Ca^{2+} influx or steady-state $[Ca^{2+}]_i$ levels,[2] despite a consistent 18–32% reduction in Ca^{2+}-pump V_{max}.

To see if the above changes on deoxygenation could be due solely to increased Ca^{2+} influx, or whether Ca^{2+} pump inhibition played a role, we developed pump-leak kinetic models that fit the oxy curve, and tested whether changes in the Ca^{2+} leak alone would allow them to fit the deoxy curve, or if changes in pump fluxes were also required. The results of such an analysis are shown in Fig. 4. The equation used to fit pump-leaks was of the general form

$$d[Ca_T]_i/dt = \phi_L - \phi_P \quad (1)$$

where ϕ_L and ϕ_P are Ca^{2+} leak and pump fluxes, respectively. ϕ_L was assumed to be constant, but was allowed to fluctuate ±20% about its measured value (Table III, donor 2) during model fitting (Fig. 4). ϕ_P was of the form:

$$\phi_P = V_{max}(([Ca^{2+}]_i)^n/(([Ca^{2+}]_i)^n + K_m)). \quad (2)$$

The relation between $[Ca^{2+}]_i$ and $[Ca_T]_i$ in the benz-2-loaded RBCs, in which $[Ca^{2+}]_i \ll$ calcium bound to benz-2, was obtained from

$$[Ca^{2+}]_i = K_d[Ca_T]_i/(B_T - [Ca_T]_i) \quad (3)$$

where B_T is the total benz-2 content of the RBCs (143 μmol/(340 g Hb)) in the experiment in Fig. 4) and K_d is the Ca^{2+} dissociation constant of benz-2 (~ 50 nM, (30)). Eq. (1) was solved numerically for $[Ca_T]_i$ as a function of time, using a computer program developed ad hoc. The program first adjusted V_{max}, K_m, and n to fit best the oxy curve, and then attempted best fits of the deoxy curve by changing only ϕ_L within the allowed (±20%) range. After this it tested whether additional changes in V_{max} (3 to 25 mmol/(340 g Hb h); per reference 26), and K_m (50 nM to 5 μM), would significantly improve the curve fit and, if so, it would further explore best fit values of V_{max} and K_m.

The results of this analysis indicated that several kinetic models of the pump fitted the oxy curve well. Those kinetics could be loosely grouped in two broad categories, low Ca^{2+}-affinity, low cooperativity models with $n \leq 2$ and $K_m \geq 1$ μM (LA, *dotted lines*), and high Ca^{2+}-affinity, high cooperativity models with $n \sim 2.5$–3.5 and $K_m \sim 40$–80 nM (HA, *solid lines*). But when the leak was increased from oxy to deoxy values while maintaining the oxy-pump parameters (*dash-dotted lines*), neither model could fit the steady-state $[Ca_T]_i$ levels measured in the deoxy conditions; In relation to the measured $[Ca_T]_i$ values, LA models leveled off far too high (~ 70 μmol/(340 g Hb)) in the example of Fig. 4) and HA models too low (~ 38 μmol/(340 g Hb)). To improve the fit, a large increase

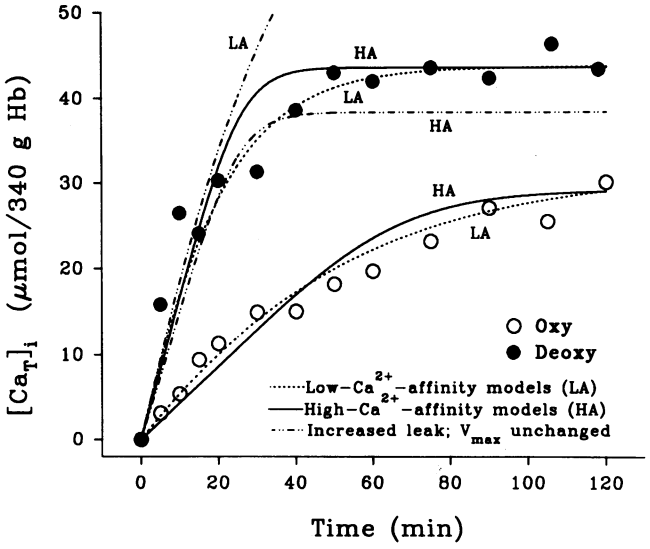

Figure 4. Effect of deoxygenation on Ca^{2+} influx and pump-leak steady-state $[Ca^{2+}]_i$ level in SS discocytes (donor 2, Table III). $[Ca_T]_i$ is plotted as a function of time in oxy and deoxy conditions. The different lines represent theoretical fits of pump-leak models with different Ca^{2+} pump kinetics (described in the text of Results). LA and HA identify the lines predicted by low and high Ca^{2+}-affinity models, respectively. The lower solid and dotted lines represent best fits in oxy conditions. Values of pump (Eq. 2) and leak parameters, in the examples chosen for this figure, are as follows. For HA pumps, K_m = 0.07 μM, n = 3.5 and V_{max} = 10 mmol/(340 g Hb h); ϕ_L was increased from 26 (oxy) to 90 (deoxy) μmol/(340 g Hb h), either with a compensating decrease in V_{max} from 10 (oxy) to 6 (deoxy) mmol/(340 g Hb h) (*HA, upper solid line*) or with V_{max} unchanged (*HA, lower dash-dotted line*). For LA pumps, K_m = 4.0 μM, n = 1 and V_{max} = 10 mmol/(340 g Hb h); ϕ_L was increased from 35 (oxy) to 120 (deoxy) μmol/(340 g Hb h), either with a compensating increase in V_{max} from 10 (oxy) to 22 (deoxy) mmol/(340 g Hb h) (*LA, upper dotted line*) or with V_{max} unchanged (*LA, upper dash-dotted line*).

2. In the recent study cited, benz-2-loaded rbc from three normal donors, suspended in autologous plasma, showed a Ca^{2+} influx (in μmol/340 g Hb) of 33±3.3 oxy and 37±4.5 deoxy ($P > 0.35$); the pump-leak steady-state $[Ca^{2+}]_i$ was 11±1.2 nM oxy and 13±1.2 nM deoxy ($P > 0.10$).

Table I. Effect of Deoxygenation on the Ca^{2+} Pump V_{max} in SS RBC Fractions

Donor	Condition	R1		R2		D	ISC
		Ca^{2+}* efflux	% Retics	Ca^{2+}* efflux	% Retics	Ca^{2+}* efflux	Ca^{2+}* efflux
	Oxy	4.0		—		8.0	5.0
1 (CW)	Deoxy	3.2	30.9	—		7.4	4.3
	(O–D)/O	−20%				−7.5%	−14%
	Oxy	6.9		14.8		12.3	7.1
2 (WR)	Deoxy	5.7	81.8	10.6	69.8	10.5	7.2
	(O–D)/O	−17%		−28%		−15%	1.4%
	Oxy	9.0		6.6		5.7	3.6
3 (EM)	Deoxy	7.5	53.5	6.2	36.1	5.2	2.6
	(O–D)/O	−17%		−6.1%		−9%	−28%
	Oxy	10.5		9.4		7.8	4.9
4 (BW)	Deoxy	9.8	12.6	7.9	6.8	6.0	4.8
	(O–D)/O	−6.7%		−16%		−23%	−2.0%

* Ca^{2+} efflux in (mmol/(340 g Hb h)). (O–D): Oxy-deoxy differences; (O–D)/O: Deoxy-induced fractional change in Ca^{2+} pump V_{max}. Mean values (±SEM) for the reticulocyte-rich (R1 + R2) fractions were 8.7±1.3 (oxy) and 7.3±1.0 (deoxy), for the discocyte fraction, 8.5±1.4 (oxy) and 7.3±1.2 (deoxy), and for the ISC-rich fraction, 5.2±0.7 (oxy) and 4.7±0.9 (deoxy). A paired t statistic indicates that the differences between the oxy and deoxy values are significant for the reticulocyte-rich fractions ($P < 0.01$) and for the discocyte fraction ($P < 0.025$) but not for the dense, ISC-rich fraction ($P > 0.05$).

in pump V_{max} was needed for the LA pump models, and a mild (20 to 50%) decrease in V_{max} for the HA pump models (Fig. 4). The correction has this inverse pattern because the response of the LA models' oxy pump to the deoxy-increase in $[Ca^{2+}]_i$ is too weak to lower the steady-state $[Ca_T]_i$ to levels near those measured unless the Ca^{2+}-pump V_{max} increases on deoxygenation. On the other hand, the oxy-pump of the HA models responds too strongly to the increase in $[Ca^{2+}]_i$ on deoxygenation, and its V_{max} requires mild inhibition to fit the observed deoxy steady-state $[Ca_T]_i$. Thus, only high affinity models are consistent with the measured V_{max} values and with the observed reductions in pump V_{max} on deoxygenation (Figs. 1–3 and Table I). However, the scatter of the experimental points in the three experiments of this series was too large to allow precise kinetic descriptions of the pump from the analysis illustrated in Fig. 4.

Table II. Effect of Deoxygenation on Cell and Suspension pH (pH_i, pH_s)

	Measured	Predicted pH_{deoxy} for given initial pH_{oxy} and indicated ΔpI
		ΔpI: 7.20 to 7.40
$pH_{s\text{-}oxy}$	7.41	7.41
$pH_{i\text{-}oxy}$	7.21	7.21
$pH_{s\text{-}deoxy}$	7.49	7.49
$pH_{i\text{-}deoxy}$	7.33	7.31
$pH_{s\text{-}deoxy} - pH_{s\text{-}oxy}$	0.08	0.08
$pH_{i\text{-}deoxy} - pH_{i\text{-}oxy}$	0.12	0.10

The extended red cell model (18) was used to estimate the change of pI (ΔpI) providing the nearest fit of the measured deoxygenation-induced pH shifts. The fractionated RBCs were suspended in solution B at Hct ~ 6%, and pH was measured at 37°C as described in Methods (note that $pH_o \sim pH_s$). The example chosen for this Table (fraction R2 of donor EM) is representative of nine similar measurements with R1, R2, and D fractions from three different patients.

Differences in cytoplasmic Ca^{2+} buffering among SS RBC subpopulations. In the experiment of Fig. 3, the higher the density of the SS RBC fraction, the lower the $([Ca_T]_i)_{Eq}$, both in oxy and deoxy conditions. Since the cell fractions were suspended at similar Hct, initial $[Ca^{2+}]_o$ and pH, their different $([Ca_T]_i)_{Eq}$ levels could reflect differences in cytoplasmic Ca^{2+} buffering, but would also be affected by differences in cell volume and proton ratios. Each of these factors was considered in the analysis of the data in Fig. 3 (oxy conditions) shown in Table IV.

The progressive decrease in cell volumes (in liters per 340 g Hb) from the lightest R1 reticulocyte-rich fraction to the dense, ISC-rich cells would contribute to a corresponding decrease in $([Ca_T]_i)_{Eq}$ (expressed per 340 g Hb) even if the total calcium contents in the density fractions (per volume RBCs) were the same. Cell volume differences can be discounted by expressing $([Ca_T]_i)_{Eq}$ per 1 cells, but conversion from the measured value of $([Ca_T]_i)_{Eq}$ per 340 g Hb requires knowledge of the mean cell volume of each density fraction. Since the distribution of cell volumes within each fraction was unknown, we considered the possible extremes within each range, as explained in the legend of Table IV. Over the full range of values which take the heterogeneity of cell volumes and proton ratios (r) into account, the ionized fraction of total cell calcium (α) increased with each cell density fraction, from reticulocytes to ISCs. Values of α similarly calculated from SS density fractions in six similar experiments are shown in Table V. Taking the two high-reticulocyte fractions (R1 and R2) together for comparisons, the results show that within each sample, the values of α in the reticulocyte-rich fractions were significantly lower than those in the discocytes or the dense SS cells. A lower fraction of ionized calcium means that the reticulocyte-rich fractions have a relatively higher Ca^{2+}-binding capacity than the other frac-

Table III. Effect of Deoxygenation on the Passive Ca^{2+} Influx and Pump–Leak Steady-State Concentrations of Calcium in SS Discocytes

Donor	Condition	$[benz\text{-}2]_i$	Ca^{2+} influx	$([Ca_T]_i)_{StSt}$	$([Ca^{2+}]_i)_{StSt}$
		(μmol/340 g Hb)	*(μmol/340 g Hb h)*	*(μmol/340 g Hb)*	*(nM)*
1 (WR)	Oxy	187	37.2	34.5±2.7	11.3±0.96
	Deoxy		153	72.5±1.7	31.7±1.3
2 (EM)	Oxy	143	34.6	26.5±1.4	11.4±0.59
	Deoxy		82.8	43.4±0.61	21.8±0.45
3 (AM)	Oxy	128	28.7	20.1±1.4	9.4±0.76
	Deoxy		112	48.0±0.74	30.0±0.75

Steady-state levels of total, $([Ca_T]_i)_{StSt}$, and free ionized calcium, $([Ca^{2+}])_{StSt}$, were determined in SS discocytes preloaded with benz-2 and suspended in autologous plasma. In each experiment, measured $[Ca_T]_i$ was plotted as a function of time (as shown for donor 2 in Fig. 4), and Ca^{2+} influx was calculated from the linear regression slope of the first four or five experimental points ($t \leq 20$ min); for each curve, the correlation coefficient was > 0.9. Each value of $([Ca_T]_i)_{StSt}$ represents the mean±SEM of four to six measurements in the "steady state" portions of the data curves such as those as shown in Fig. 4. $([Ca^{2+}]_i)_{StSt}$ was calculated for each of the data points (see Eq. 3 in Results) and the means±SEM are shown. Application of a t statistic to each set of oxy and deoxy concentration values shows that the increase in $([Ca^{2+}]_i)_{StSt}$ on deoxygenation is highly significant for each experiment ($P < 0.0005$).

tions. In three of four samples, α in the dense SS cells was substantially higher than in the discocytes, indicating a trend, but not sufficient to establish statistical significance.

Discussion

The results above show that deoxygenation of SS RBCs led to specific changes in their cytoplasmic Ca^{2+} buffering, cell pH, passive Ca^{2+} permeability, Ca^{2+} pump, and in their pump-leak steady-state $[Ca^{2+}]_i$ levels. In addition, regardless of their oxygenation state, the various SS RBC density fractions showed differences in residual Ca^{2+} retention after brief Ca^{2+} loads, and in their cytoplasmic Ca^{2+} buffering. These results and differences are analyzed below.

Differences in cytoplasmic Ca^{2+} buffering among SS RBC subpopulations. When normal RBCs are loaded in vitro with nonphysiological Ca^{2+} levels above ~ 10 μmol/(340 g Hb), the cytoplasmic calcium is loosely bound, as if there were a single, large capacity, low affinity Ca^{2+} buffer (19), with 12 to 35% of the total cell calcium in the ionized form (α = 0.12–0.35; reference 37). Available evidence suggests that the main low affinity Ca^{2+} buffer is Hb (38), with additional buffering by organic and inorganic phosphates (20). Previous measurements of α in unfractionated SS RBCs gave values within the range for normal RBCs (16). The results in Tables IV and V suggest that within each SS blood sample, the Ca^{2+} binding capacity of the reticulocytes exceeds those of the more mature discocytes and of the dense cells. Since the ionophore permea-

Table IV. Analysis of Differences in Cytoplasmic Ca^{2+} Buffering in SS RBC Density Fractions

Density fraction	Hct	V_r	$([Ca_T]_i)_{Eq}$		$([Ca^{2+}]_o)_{Eq}$	r^2/α	r	r^2	α (range)
	%		*μmol/340 g Hb*	*μmol/l cells*	*μM*				
R1	9.10	1.07	938	877	22.2	39.5	1.58	2.51	0.064 (0.062–0.068)
R2	8.38	1.01	843	835	32.8	25.5	1.58	2.51	0.099 (0.096–0.101)
D	7.57	0.85	686	807	42.1	19.2	1.70	2.88	0.15 (0.13–0.18)
ISC	8.03	0.75	539	719	45.9	15.7	2.00	4.00	0.26 (0.25–0.26)

V_r is defined as the mean RBC volume within each density fraction, expressed relative to the volume of a "normal" RBC with an MCHC of 34 g/dl (340 g/liter packed cells). V_r was calculated in RBC fractions with mean densities of 1.084 (R1), 1.089 (R2), 1.105 (D) and 1.120 (ISC), using previously reported relationships between density and cell volumes (8), based on the specific volume of Hb of 0.74 ml/g Hb (8, 57). With V_r, the measured $([Ca_T]_i)_{Eq}$ per 340 g Hb can be expressed per liter cells, using: $([Ca_T]_i)_{Eq}$ (per l cells) = $([Ca_T]_i)_{Eq}$ (per 340 g Hb)/V_r. This is needed to calculated $([Ca^{2+}]_o)_{Eq}$, from: $([Ca^{2+}]_o)_{Eq} = [Ca_T]_s$ − Hct $([Ca_T]_i)_{Eq}$ (per l cells))/(1-Hct). From this, r^2/α and α can be calculated as described in Methods. The values used for the proton ratios (r) for fractions R1, R2, and D were derived from direct measurements of cell and medium pH (as shown for the same sample's fraction R2 in Table II). The r value for the ISC fraction was taken as the mean of several previous measurements, ranging between 1.90 to 2.12 (7). The range of α values given in parenthesis was obtained using two extreme density values for each fraction: 1.080 and 1.087 for R1, 1.087 and 1.091 for R2, 1.091 and 1.118 for D, and 1.118 and 1.125 for ISCs. Note that the measured values of $([Ca_T]_i)_{Eq}$ expressed as μmol/(340 g Hb) are taken from the experiment shown in Figs. 1 and 3 (oxy RBC only), and error bars are shown in Fig. 3.

Table V. Ionized Fraction of Cytoplasmic Ca^{2+} (α) in Oxygenated SS RBC Density Fractions

Donor		R	D	ISC	D-R	ISC-R	ISC-D
EM	R1	0.064	0.15	0.26	0.086	0.20	0.11
	R2	0.099			0.051	0.16	
BW	R1	0.17	0.30	0.31	0.13	0.14	0.010
	R2	0.19			0.11	0.12	
WR			0.15	0.29			0.14
EM2	R2	0.24		0.38		0.14	
BB	R1	0.43		0.67		0.24	
RD			0.28	0.65			0.37
MEAN		0.199	0.220	0.427	0.094	0.166	0.158
SEM		0.053	0.041	0.076	0.017	0.018	0.076
P					< 0.005	< 0.0005	> 0.05

This table summarizes all measurements of α in RBC density fractions from six separate blood samples from five SS donors, calculated from data such as that shown for donor EM in Table IV. R1, R2, D, and ISC refer to the density fractions described in the text. For the purposes of this analysis, both reticulocyte-rich density fractions, R1 and R2, are listed together under column R. The paired differences between α values of different fractions from the same sample are shown (columns D-R, ISC-R, and ISC-D) and the significance of the differences tested using a paired *t* statistic.

bilizes the membranes of organelles and endocytic vesicles as well as cells, we cannot distinguish between the contribution of cytosolic and organelle components to the higher Ca^{2+} binding of the reticulocyte-rich SS cell fractions.

Previous findings that the dense ISC-rich fractions of SS RBCs have relatively low concentrations of 2,3-diphosphoglyceric acid (2,3-DPG; reference 7), the main organic phosphate buffer of Ca^{2+}, may help explain the relatively low Ca^{2+} buffering (high α) observed in this cell fraction.

Effects of deoxygenation on cytoplasmic Ca^{2+} buffering. For all density fractions of SS RBCs, $([Ca_T]_i)_{Eq}$ was lower in the deoxy than in the oxy suspensions (Figs. 1–3). A similar observation in AA RBCs (18) was explained by changes in both the proton ratio (r), which determines the equilibrium partition of $[Ca^{2+}]_o$ and $[Ca^{2+}]_i$, and in the ionized fraction of cell calcium, α, which reflects Ca^{2+} buffering. The change in r on RBC deoxygenation can be calculated from measurements of cell and medium pH. For instance, from the pH values in Table II (for fraction R2, donor EM):

$$r_{oxy} = 10^{pH_{s\text{-}oxy} - pH_{i\text{-}oxy}} = 10^{7.41-7.21} = 1.58,$$

$$r_{oxy}^2 = 2.51;$$

$$r_{deoxy} = 10^{pH_{s\text{-}deoxy} - pH_{i\text{-}deoxy}} = 10^{7.49-7.33} = 1.45, \quad \text{and}$$

$$r_{deoxy}^2 = 2.09.$$

For the same fraction and donor in the experiment of Fig. 3, α (calculated as described in Methods) was 0.099 in oxy (Table IV) and 0.13 in deoxy conditions. Similar differences were obtained with other SS RBC density fractions (not shown). Thus the deoxygenation-induced fall in $([Ca_T]_i)_{Eq}$ apparently results from both a reduced proton ratio and decreased cytoplasmic Ca^{2+} binding (increased α). Further attempts at more quantitative analysis are not justified, because of the heterogeneities within each SS RBC density fraction.

These results indicate that like AA RBCs (18), SS RBCs bind less Ca^{2+} in deoxy than in oxy conditions, and the reduced binding may result from increased protonation of deoxy-Hb and/or its increased binding of organic phosphates.

Ca^{2+} pump V_{max} in density-fractionated SS RBCs. In the present studies, the Ca^{2+} pump V_{max} of the oxy SS cells from different donors and their density-fractions showed only moderate variation (between about 4 and 12 mmol/(340 g Hb)); the only pattern evident was a tendency for a lower V_{max} with the dense SS cells than with the discocytes from the same samples (Figs. 1 and 2, Table I); since our recent measurements of the passive Ca^{2+} influxes in SS reticulocyte and discocyte fractions also showed little differences (2), it would appear that the pump-leak Ca^{2+} turnover changes little during the maturation of the SS reticulocytes.

These results appear to differ from earlier measurements by Wiley and Shaller (39) on blood samples from diverse patients with reticulocytosis, which suggested that the Ca^{2+} permeability of AA reticulocytes was over 40-fold that in mature RBCs. Concomitant findings of no increase in total RBC calcium in the high-reticulocyte samples carried the implication that the reticulocytes' steady-state Ca^{2+} pumping (not measured directly) had to be proportionately high to balance the increased leaks. At first, those findings seemed consistent with the pattern of decreasing transporter activity and ionic traffic during RBC maturation which had been well documented for Na-pump and K:Cl-mediated transport in RBCs from different species (40–43). But further considerations raise the possibility that the increased passive Ca^{2+} influx in high-reticulocyte AA RBC suspensions might have resulted from the experimental conditions. The present studies employed Ca^{2+} chelators, which can be incorporated nondisruptively into intact cells (30), allowing subsequent measurement of passive Ca^{2+} fluxes in metabolically competent RBCs with functional pumps (see Fig. 4). Before the synthesis of these Ca^{2+} chelators, such fluxes were measured in cells whose Ca^{2+} pumps were inhibited by ATP depletion. It is possible that the different conditions of Wiley and Shaller's measurements, which included ATP deple-

tion, may have caused the markedly increased Ca^{2+} leak they observed in reticulocytes.

The results described here suggest that by the reticulocyte stage, the expression and function of the Ca^{2+} pump is already set at the levels found in mature RBCs. The absence of high Ca^{2+} turnover in the reticulocytes would be understandable if passive Ca^{2+} dissipators did not participate in cell signaling beyond the erythroblast stage. By contrast, the gradual decline in the activity of transporters which dissipate Na^+ and K^+ gradients may reflect their continued need during reticulocyte maturation, both for volume regulation and to provide essential substrates for metabolism and protein synthesis. It seems unlikely that such an explanation would apply only to SS cells. In view of the uncertainties concerning Ca^{2+} transport in AA reticulocytes, and the present results in SS RBCs, further experiments will be needed to reassess the state of Ca^{2+} transport during AA RBC maturation.

Measurements of the Ca^{2+} pump V_{max} in the SS RBC density fractions from four donors revealed that in each case, there was slight inhibition of the Ca^{2+} pump in the dense, ISC-rich fraction as compared with the discocytes (Table I). This may be related to differences in $[Mg^{2+}]_i$ and $[Mg^{2+}]_i/[ATP]_i$ ratios in these SS subpopulations, as discussed below.

Effects of deoxygenation on Ca^{2+} pump V_{max}. Recent studies showed that in AA RBCs, deoxygenation reduced the V_{max} of the Ca^{2+} pump by 18–32%,[3] and that the inhibition was not explained by the deoxy-shifts in cell pH (18). Similar measurements in a larger number of oxygenated fresh normal RBC showed a wide variation in saturated Ca^{2+} pump effluxes, between 4 and 25 mmol/(l cells/h), (26). The V_{max} values were highly reproducible within each RBC sample, but was very variable among different samples, even from the same donor on different days. The variability suggested the operation of factors that control the fraction of active pumps, the pump turnover, or both, as discussed below. Those results justified comparisons of experimental conditions on the V_{max} of RBC from the same sample (e.g., deoxygenation), but comparisons of values among different samples must acknowledge these normal variations. Thus the V_{max} values found in all SS cell fractions were well within the range observed in normal RBC.

In the present experiments, SS RBC Ca^{2+} pumps were also inhibited on deoxygenation. With the exception of the dense fractions, in which the inhibition was minimal or absent in two of the four samples and oxy–deoxy differences were not significant, the Ca^{2+} pump inhibition on deoxygenation ranged between 7 and 28%, and was statistically significant for the reticulocyte-rich fractions and the discocyte fraction. However, the extent of Ca^{2+} pump inhibition did not correlate with either the density fraction or the proportion of reticulocytes, and varied considerably among the donors (Table I).

These marked variations among SS RBC fractions and donors suggest that deoxygenation affects the Ca^{2+} pump indirectly, through pump controlling factors in SS cells that may vary among both individuals and their RBC subpopulations, i.e., Mg^{2+}, 2,3-DPG, and ATP. $[Mg^{2+}]_i$ is a cofactor essential for pump dephosphorylation at physiological levels of ATP (44). Upon deoxygenation of RBCs, $[Mg^{2+}]_i$ increases substantially (45–48); this increase is most dramatic in dense, ISC-rich SS RBC fractions, in which the normal inward electrochemical gradient of Mg^{2+} is reversed on deoxygenation (7). The main phosphate compounds which bind Mg^{2+} are 2,3-DPG and ATP; due to their increased binding to deoxy-Hb, their availability for Mg^{2+} buffering decreases on RBC deoxygenation with consequent increase in $[Mg^{2+}]_i$ (45–48). The total cell contents of Mg^{2+}, 2,3-DPG, and ATP vary among SS cell subpopulations; they are all highest in the lightest reticulocyte-rich fractions and lowest in the dense ISC-rich fractions (7); 2,3-DPG content in particular is very low in dense SS RBCs, with large variations among donors (7).

In addition, a $[Mg^{2+}]_i/[ATP]_i$ ratio near one is optimal for Ca^{2+}-Mg^{2+}-ATPase and $Na^+ + K^+$-ATPase activities, with inhibition at higher and lower ratios (49–51). Hence, differences in this ratio may contribute to the observed variations in Ca^{2+} pump V_{max} among RBCs from different SS donors and among the SS RBC subpopulations, before and after deoxygenation. However, further studies relating intracellular Mg^{2+} and nucleotide levels to Ca^{2+} pump activity (such as those attempting to explain the Na^+ pump inhibition in dense SS cells (7)) will be needed to test this possibility.

Deoxygenation-induced increase in $[Ca^{2+}]_i$ in SS discocytes: implication for SS RBCs dehydration, and contributions of Ca^{2+} leak and pump. The present experiments document for the first time that full deoxygenation of SS discocytes increases $[Ca^{2+}]_i$ from physiological levels of $\sim$ 10 nM to mean values of 20–30 nM. The threshold for activating Ca^{2+}-sensitive K channels in normal RBCs was examined by Tiffert et al. (52), who raised Ca^{2+} influx into normal RBCs in small steps (using low A23187 concentrations), and showed that with $[Ca^{2+}]_i$ levels estimated at $\sim$ 40 nM, a fraction of dehydrated, dense cells formed within 1 or 2 h of incubation at 37°C. Those measurements were made in metabolically replete, intact RBCs in order to approximate physiological conditions, but the precise kinetics of the K channel have yet to be determined in such conditions.

In assessing the pathophysiological relevance of the deoxy-induced increase in $[Ca^{2+}]_i$ in SS discocytes, however, we should recognize that they are unlikely to become fully deoxygenated in vivo, and the extent of their Ca^{2+} permeabilization on partial deoxygenation is unknown. While the fraction of Hb S polymer formed at partial levels of RBC oxygen saturation has been measured (53, 54), the relation between the extent and organization of the Hb S polymers in the SS RBC subpopulations and increased Ca^{2+} permeability is unknown. Further studies are needed to help predict whether the increased Ca^{2+} influx observed here occurs in vivo, or only represents maximal values for fully deoxygenated SS discocytes.

It should also be recognized that even after density-fractionation, the SS discocyte fraction is heterogeneous; it includes at least one subpopulation of reticulocytes on a fast dehydration track, traversing the density stage of discocytes (2). The observed deoxy increase in $[Ca^{2+}]_i$ is a mean value, and it is very likely that in some of these deoxygenated SS cells, $[Ca^{2+}]_i$ exceeds the activation threshold of Ca^{2+}-sensitive K channels ($\sim$ 40 nM $[Ca^{2+}]_i$) which can rapidly dehydrate AA cells (52). In the circulation, however, sickling and Ca^{2+} permeabilization would probably be intermittent, and dehydration by this mechanism should then be much slower than in experimental

3. In that recent study of normal RBC, V_{max} of the Ca^{2+} pump in five blood samples was (in mmol/340 g Hb±SEM) 14.0±1.4 in the oxy and 10.5±0.8 in the deoxy cells. Statistical (paired t) analysis gave $P < 0.005$.

conditions with sustained channel activation. In any case, the present results establish that deoxygenation of SS cells can indeed generate $[Ca^{2+}]_i$ levels that activate Ca^{2+}-sensitive K^+ channels.

The analysis in Fig. 4 indicated that the observed deoxygenation-induced rise in $[Ca^{2+}]_i$ could not be explained by the increased Ca^{2+} permeability alone; it was also necessary to postulate changes in pump V_{max}. Two kinetic pump-models were considered, with high or low Ca^{2+} affinity, and opposite changes in their V_{max} were required to fit the data. But for the low affinity model, the large increases in pump V_{max} needed to fit the deoxy conditions were inconsistent with the experimental observations that deoxygenation inhibited the V_{max} of SS discocytes (Table I). The kinetic properties of the pump at physiological $[Ca^{2+}]_i$ levels corresponds to a high Ca^{2+}-affinity, high V_{max} pump with marked sigmoidicity in the shape of the activation curve with increasing $[Ca^{2+}]_i$ (30), comparable to that described by Kosk-Kosicka et al. (55, 56) for pump oligomers. These considerations suggest that V_{max} inhibition of high Ca^{2+}-affinity Ca^{2+} pumps contributes to the increased $[Ca^{2+}]_i$ after deoxygenation of SS cells.

Acknowledgments

We wish to thank the National Institutes of Health (USA, grants HL-28018 and HL-21016) and the Wellcome Trust (UK) for funds.

References

1. Bertles, J. F., and P. F. A. Milner. 1968. Irreversibly sickled erythrocytes: a consequence of the heterogeneous distribution of hemoglobin types in sickle cell anemia. *J. Clin. Invest.* 47:1731–1741.

2. Bookchin, R. M., O. E. Ortiz, and V. L. Lew. 1991. Evidence for a direct reticulocyte origin of dense red cells in sickle cell anemia. *J. Clin. Invest.* 87:113–124.

3. Lew, V. L., and R. M. Bookchin. 1992. Role of reticulocyte transport heterogeneity in the generation of mature sickle cells with different volumes. *Biochem. Soc. Trans.* 40:797–800.

4. Tosteson, D. C., E. Carlsen, and E. T. Dunham. 1955. The effects of sickling on ion transport I. Effect of sickling on potassium transport. *J. Gen. Physiol.* 39:31–53.

5. Tosteson, D. C. 1955. The effects of sickling on ion transport II. The effect of sickling on sodium and cesium transport. *J. Gen. Physiol.* 39:55–67.

6. Bookchin, R. M., and V. L. Lew. 1981. Effect of a 'sickling pulse' on calcium and potassium transport in sickle cell trait red cells. *J. Physiol.* 312:265–280.

7. Ortiz, O. E., V. L. Lew, and R. M. Bookchin. 1990. Deoxygenation permeabilizes sickle cell anaemia red cells to magnesium and reverses its gradient in the dense cells. *J. Physiol.* 427:211–226.

8. Lew, V. L., C. J. Freeman, O. E. Ortiz, and R. M. Bookchin. 1991. A mathematical model on the volume, pH and ion content regulation of reticulocytes. Application to the pathophysiology of sickle cell dehydration. *J. Clin. Invest.* 87:100–112.

9. Eaton, J. W., T. D. Skelton, H. S. Swofford, C. E. Koplin, and H. S. Jacob. 1973. Elevated erythrocyte calcium in sickle cell disease. *Nature (Lond.).* 246:105–106.

10. Palek, J. 1973. Calcium accumulation during sickling of haemoglobin S red cells. *Blood.* 42:988–1000.

11. Bookchin, R. M., C. Raventos, and V. L. Lew. 1981. Abnormal vesiculation and calcium transport by "one-step" inside-out vesicles from sickle cell anemia red cells. Comparisons with transport by intact cells. *In* The Red Cell: Fifth Ann Arbor Conference. G. J. Brewer, editor. Alan R. Liss, New York. 163–182.

12. Lew, V. L., A. Hockaday, M. I. Sepulveda, A. P. Somlyo, A. V. Somlyo, O. E. Ortiz, and R. M. Bookchin. 1985. Compartmentalization of sickle cell calcium in endocytic inside-out vesicles. *Nature (Lond.).* 315:586–589.

13. Bookchin, R. M., O. E. Ortiz, A. V. Somlyo, A. P. Somlyo, M. I. Sepulveda, A. Hockaday, and V. L. Lew. 1985. Calcium-accumulating inside-out vesicles in sickle cell anemia red cells. *Trans. Assoc. Am. Phys.* 98:10–20.

14. Williamson, P., E. Puchulu, J. T. Penniston, M. P. Westerman, and R. A. Schlegel. 1992. Ca^{2+} accumulation and loss by aberrant endocytic vesicles in sickle erythrocytes. *J. Cell. Physiol.* 152:1–9.

15. Harrison, D. G., and C. Long. 1968. The calcium content of human erythrocytes. *J. Physiol.* 199:367–381.

16. Bookchin, R. M., and V. L. Lew. 1980. Progressive inhibition of the Ca pump and Ca:Ca exchange in sickle red cells. *Nature (Lond.).* 284:561–563.

17. Rhoda, M. D., M. Apovo, Y. Beuzard, and F. Giraud. 1990. Ca^{2+} permeability in deoxygenated sickle cells. *Blood.* 75:2453–2458.

18. Tiffert, T., Z. Etzion, R. M. Bookchin, and V. L. Lew. 1993. Effects of deoxygenation on active and passive Ca^{2+} transport and cytoplasmic Ca^{2+} buffering in normal human red cells. *J. Physiol.* 464:529–544.

19. Ferreira, H. G., and V. L. Lew. 1976. Use of ionophore A23187 to measure cytoplasmic Ca buffering and activation of the Ca pump by internal Ca. *Nature (Lond.).* 259:47–49.

20. Lew, V. L., and A. M. Brown. 1979. Experimental control and assessment of free and bound calcium in the cytoplasm of intact mammalian red cells. *In* Detection and Measurement of Free Ca in Cells. C. C. Ashley and A. K. Campbell, editors. Elsevier/North-Holland, Amsterdam. 423–432.

21. Lew, V. L., and J. García-Sancho. 1989. Measurement and control of intracellular calcium in intact red cells. *In* Methods in Enzymology, Vol. 173, Biomembranes, Part T, Cellular and Subcellular Transport: Eukaryotic (Nonepithelial) Cells. S. Fleischer and B. Fleischer, editors. Academic Press, Inc., San Diego, CA. 100–112.

22. Corash, L. M., S. Piomelli, H. C. Chen, C. Seaman, and E. Gross. 1974. Separation of erythrocytes according to age on a simplified density gradient. *J. Lab. Clin. Med.* 84:147–151.

23. Ortiz, O. E., V. L. Lew, and R. M. Bookchin. 1986. Calcium accumulated by sickle cell anemia red cells does not affect their potassium (^{86}Rb) flux components. *Blood.* 67:710–715.

24. Lew, V. L., and L. O. Simonsen. 1980. Ionophore A23187-induced calcium permeability of intact human red blood cells. *J. Physiol.* 308:60P.

25. Lew, V. L., and L. O. Simonsen. 1981. A23187-induced ^{45}Ca-flux kinetics reveals uniform ionophore distribution and cytoplasmic calcium buffering in ATP-depleted human red cells. *J. Physiol.* 316:6P–7P.

26. Dagher, G., and V. L. Lew. 1988. Maximal calcium extrusion capacity and stoichiometry of the human red cell calcium pump. *J. Physiol.* 407:569–586.

27. Pressman, B. C. 1976. Biological applications of ionophores. *Annu. Rev. Biochem.* 45:501–530.

28. García-Sancho, J., and V. L. Lew. 1988. Detection and separation of human red cells with different calcium contents following uniform calcium permeabilization. *J. Physiol.* 407:505–522.

29. García-Sancho, J., and V. L. Lew. 1988. Heterogeneous calcium and adenosine triphosphate distribution in calcium-permeabilized human red cells. *J. Physiol.* 407:523–539.

30. Lew, V. L., R. Y. Tsien, C. Miner, and R. M. Bookchin. 1982. Physiological $[Ca^{2+}]_i$ level and pump-leak turnover in intact red cells measured using an incorporated Ca chelator. *Nature (Lond.).* 298:478–481.

31. Tiffert, T., J. García-Sancho, and V. L. Lew. 1984. Irreversible ATP depletion caused by low concentrations of formaldehyde and of calcium-chelator esters in intact human red cells. *Biochim. Biophys. Acta.* 773:143–156.

32. Orringer, E. P., and W. D. Mattern. 1976. Formaldehyde-induced hemolysis during chronic hemodialysis. *N. Engl. J. Med.* 294:1416–1420.

33. García-Sancho, J. 1985. Pyruvate prevents the ATP depletion caused by formaldehyde or calcium-chelator esters in the human red cell. *Biochim. Biophys. Acta.* 813:148–150.

34. García-Sancho, J., and V. L. Lew. 1988. Properties of the residual calcium pools in human red cells exposed to transient calcium loads. *J. Physiol.* 407:541–556.

35. Bunn, H. F., and M. McDonough. 1974. Asymmetrical hemoglobin hybrids. An approach to the study of subunit interactions. *Biochemistry* 13:988–983.

36. Bunn, H. F., and B. G. Forget. 1986. Hemoglobin: Molecular, Genetic and Clinical Aspects. W. B. Saunders Company, Philadelphia.

37. Simonsen, L. O., J. Gomme, and V. L. Lew. 1982. Uniform ionophore A23187 distribution and cytoplasmic calcium buffering in intact human red cells. *Biochim. Biophys. Acta.* 692:431–440.

38. Schatzmann, H. J. 1973. Dependence on calcium concentration and stoichiometry of the calcium pump in human red cells. *J. Physiol.* 235:551–569.

39. Wiley, J. S., and C. C. Shaller. 1977. Selective loss of calcium permeability on maturation of reticulocytes. *J. Clin. Invest.* 59:1113–1119.

40. Rapoport, S. M. 1986. The Reticulocyte. CRC Press, Boca Raton, FL. 238 pp.

41. Blostein, R., and E. Grafova. 1990. Decrease in Na^+-K^+-ATPase associated with maturation of sheep reticulocytes. *Am. J. Physiol.* 259:C241–C250.

42. Lauf, P. K. 1985. K+:Cl− cotransport: Sulfhydryls, divalent cations, and the mechanism of volume activation in a red cell. *J. Membr. Biol.* 88:1–13.

43. Lauf, P. K., J. Bauer, N. C. Adragna, H. Fujise, A. M. M. Zade-Oppen, K. H. Ryu, and E. Delpire. 1992. Erythrocyte K-Cl cotransport: Properties and regulation. *Am. J. Physiol. Cell Physiol.* 263:C917–C932.

44. Garrahan, P. J., and A. F. Rega. 1986. The Ca^{2+} pump of plasma membranes. CRC Press, Boca Raton.

45. Bunn, H. F., B. J. Ransil, and A. Chao. 1971. The interaction between erythrocyte organic phosphates, magnesium ion, and hemoglobin. *J. Biol. Chem.* 246:5273–5279.

46. Berger, H., G. R. Janig, G. Gerber, K. Ruckpaul, and S. M. Rapoport. 1973. Interaction of haemoglobin with ions. Interactions among magnesium, adenosine 5′-triphosphate, 2,3-biphosphoglycerate, and oxygenated and deoxygenated human haemoglobin under simulated intracellular conditions. *Eur. J. Biochem.* 38:553–562.

47. Gerber, G., H. Berger, G. R. Janig, and S. M. Rapoport. 1973. Interaction of haemoglobin with ions. Quantitative description of the state of magnesium, adenosine 5′-triphosphate, 2,3-biphosphoglycerate, and human haemoglobin under simulated intracellular conditions. *Eur. J. Biochem.* 38:563–571.

48. Flatman, P. W. 1980. The effect of buffer composition and deoxygenation on the concentration of ionized magnesium inside human red blood cells. *J. Physiol.* 300:19–30.

49. Dunham, E. T., and I. M. Glynn. 1961. Adenosinetriphosphatase activity and the active movements of alkali metal ions. *J. Physiol.* 156:274–293.

50. Flatman, P. W., and V. L. Lew. 1981. The magnesium-dependence of sodium-pump-mediated sodium-potassium and sodium-sodium exchange in intact human red cells. *J. Physiol.* 315:421–446.

51. Flatman, P. W., and V. L. Lew. 1980. Excess magnesium converts red cell (Na + K)ATPase to the K-phosphatase. *J. Physiol.* 307:1–8.

52. Tiffert, T., J. L. Spivak, and V. L. Lew. 1988. Magnitude of calcium influx required to induce dehydration of normal human red cells. *Biochim. Biophys. Acta* 943:157–165.

53. Noguchi, C. T., D. A. Torchia, and A. N. Schechter. 1983. Intracellular polymerization of sickle hemoglobin: effects of cell heterogeneity. *J. Clin. Invest.* 72:846–852.

54. Noguchi, C. T., and A. N. Schechter. 1985. Sickle hemoglobin polymerization in solution and in cells. *Annu. Rev. Biophys. Biophys. Chem.* 14:239–263.

55. Kosk-Kosicka, D., and T. Bzdega. 1988. Activation of the erythrocyte Ca^{2+}-ATPase by either self-association or interaction with calmodulin. *J. Biol. Chem.* 263:18184–18189.

56. Kosk-Kosicka, D., T. Bzdega, A. Wawrzynow, S. Scaillet, K. Nemcek, and J. D. Johnson. 1990. Erythrocyte Ca^{2+}-ATPase: activation by enzyme oligomerization versus by calmodulin. *In* Calcium binding proteins in normal and transformed cells. R. Pochet, E. M. Lawson, and C. W. Heizmann, editors. Plenum Publishing Corporation, New York. 169–174.

57. Bureau, M., and R. Banerjee. 1976. Structure-volume relationships in hemoglobin. A densitometric and dilatometric study of the oxy leads to deoxy transformation. *Biochimie.* 58:403–407.